Influence of the Flame Straightening Process on Microstructural, Mechanical and Fracture Properties of S235 JR, S460 ML and S690 QL Structural Steels

R. Lacalle & J.A. Álvarez & D. Ferreño & J. Portilla & E. Ruiz & B. Arroyo & F. Gutiérrez-Solana

LADICIM, University of Cantabria, ETS de Ingenieros de Caminos Canales y Puertos, Av/Los Castros s/n, 39005 Santander, Spain
e-mail: ferrenod@unican.es

Abstract

The flame straightening of steel components is based on heating a local region of the part by means of a torch in order to induce a permanent deformation through a field of residual stresses. Although this is a very common practice, it is not devoid of serious drawbacks. In this paper, the influence of the flame bending procedure on the microstructure of three very different structural steels (S235 JR, S460 ML and S690 QL, respectively), widely used for the construction of metallic structures, is analysed. The consequences of the heat treatment on the mechanical and fracture properties were characterised through micro-hardness Vickers and Charpy impact tests; in addition, some elastic-plastic fracture tests were performed on precracked Charpy specimens manufactured with the S235 JR steel. The relationship between the microstructural features and the material mechanical and fracture behaviour was studied in depth in all cases, correlating the changes induced by the flame heat treatment on the microstructure with the macroscopic mechanical and fracture response. For a proper understanding of the microstructural consequences of this straightening heat treatment, it was necessary to develop a Finite Element numerical model. Based on the experimental results, this study has revealed that the consequences of the flame straightening on the microstructure, mechanical or fracture behaviour strongly depend on the nature of the material; for this reason, it is not possible to establish general recommendations. Nevertheless, the paper proposes a series of guidelines for good practice for steels similar to those characterised here.

Keywords: Flame straightening, S235 JR, S460 ML, S690 QL, Microstructure, Mechanical and fracture properties

Introduction

The flame straightening (or flame bending) technique is widely used for the control of geometric distortions or tolerance deviations in steel parts caused by the manufacturing or welding processes; it is also used to repair damaged elements. In all these cases, when a final geometry not fulfilling allowable tolerances is obtained, local reheating following predefined patterns is applied with a torch. During the heating, the material heat expansion is restricted, whether internally (due to the non-uniform temperature distribution in the material) or externally (as a consequence of applied loads or boundary constraints). As the material cools down, shrinkage occurs in the previously expanded regions, thus creating a distribution of residual stresses leading—if the process is correctly applied—to the desired permanent deformation of the component.

Flame straightening is a very common practice in structural elements fabricated with steel; nevertheless, many aspects of the process remain as uncertainties: for example, what are the optimum heating sequences and patterns, how should constraints be utilised or how to evaluate the residual stresses after heating and cooling. As Professor Avent has emphasised [1–5], "the process remains more of an art than a science". Indeed, the technical background in the workshops of steel

constructors is usually based only on empirical knowledge (if existing at all). This situation often leads to expensive and unsafe "trial-and-error" processes.

The question of the effects induced by the heating process on the microstructure and, as a consequence, on the mechanical and fracture properties is currently also an important open issue. In particular, in the case of modern high-strength steels, an excess of temperature and / or heating time may have detrimental effects on the strength and / or toughness [1–5]. The present contribution analyses the influence of the flame bending procedure on the material properties of three very different structural steels (S235 JR, S460 ML and S690 QL, respectively), widely used for the construction of metallic structures for buildings or bridges. First, the microstructural and metallurgical changes induced by the flame heating were studied; then, the mechanical properties were assessed through micro-hardness Vickers and tensile tests. Finally, the influence of the bending process on the fracture properties was determined by means of Charpy impact tests (moreover, for the sake of completeness, some additional elastic-plastic fracture tests were performed on precracked Charpy specimens manufactured in S235 JR steel).

Description of the Heat Straightening Process.

Objectives of the Research

Flame straightening is a common practice in structural steels usually applied in workshops although it is sometimes performed on site. For instance, it is used to accurately adjust elements to be subsequently connected by welding or bolting. It may also be applied to repair in-service damaged elements (for example, beams excessively distorted in a bridge or rails in a railway) without dismantling the whole structure. Moreover, applications may also be found in the steel production process itself in order to correct certain geometric defects of profiles, which are not easily modified with the press.

The flame straightening of a structural steel component is based on applying, by means of a torch, a superficial local heating in a limited region of the part. This results in a transient temperature field that generates a thermal gradient through the thickness. The region least heated in the thickness, far from the flame, restrains the free deformation of the superficial material and induces the formation of negative plastic strains in the regions of high temperatures. Additional constraints or loads can be applied on the component in order to enhance the formation of plastic strains. The combination of plastic strains and the corresponding balancing elastic strains through the thickness results in a distribution of residual stresses and, as a consequence, in the permanent deformation of the component.

The parameters of the process are selected according to the original geometry and the final shape to be achieved in the structural element. In this sense, the choice of type, location and sequence of the heating patterns, the heat input and the heating times are governed by the distortion to be straightened or the deformation to be induced. Two kinds of fuels are typically used for flame straightening, oxyacetylene or propane. The former is preferred by many users because the transference of the heat to the material is better than the propane flame, due to its higher temperature (approximately ~3200 °C vs. ~2700 °C, respectively). In any case, the heat flux is controlled to avoid temperatures in the material beyond a limit that could induce irreversible microstructural transformations: this limit is typically considered to be in the range 700–750 °C. These changes can have a major influence on the mechanical behaviour of the material [1–5]. Nevertheless, it is not possible to determine a priori which will be the consequences of the heat straightening on a specific steel; in this sense, in [2] it can be read: "hot mechanical straightening is an unproven method which may lead to damaged or degraded steel [...]". The results of this process are highly unpredictable and may result in fracture during straightening, severe changes in molecular structure which may not be reversible, severe changes in mechanical properties including a high degree of brittleness, buckles, wrinkles, crimps, and other distortions".

A large number of contributions can be found in the scientific literature focused on analysing the microstructural, mechanical or fracture properties of different steels subjected to diverse heat treatments (see, for example [6–9]). Nevertheless, to the knowledge of the authors of the present paper, little research has specifically addressed the influence of the flame bending technique on the microstructure and mechanical properties of steels. On the other hand, there are no previous studies to determine the consequences of the flame straightening on the material fracture properties or to correlate the microstructure with the mechanical or fracture responses. For these reasons, the experimental scope of the present contribution (which is described in detail below) was designed with the purpose of analysing the influence of the heat

straightening process on three very different structural steels: S235 JR, SA460 ML and S690 QL. The final goal is to delimit the possible influences of the process on the material properties.

In order to fully understand the microstructural changes that take place in the material as a consequence of the surface heating caused by the flame, a Finite Elements (FE) numerical model was developed. Only through a numerical technique is it possible to take into account the many factors participating in the process (material properties, heat flux of the flame, trajectory and speed of the torch, location of the material point to be analysed, etc.). Indeed, other factors equal, every point located below the flame in the thickness of the component will be subjected to a specific heat treatment as the evolution of its temperature over time will strongly depend on the depth of the point considered. Thus, the heating rate, the maximum temperature and the cooling rate will depend on the material point to be considered: all these parameters are of importance in elucidating the microstructural features in the heat treated steels.

Materials, Experimental and Numerical Techniques

Materials

The three following structural steel grades [10–12] were studied in this research: S235 JR, S460 ML and S690 QL. The microstructure of S235 JR and S460 ML consists of ferrite and perlite whereas S690 QL steel shows a microstructure of bainite and tempered bainite. The specified chemical compositions of the steels [10–12] are included in Table 1. As can be appreciated, the three materials selected for the research are representative of a wide range of structural steels, both from the point of view of their microstructure and their chemistry. Moreover, their mechanical and fracture behaviours are also noticeably different. S235 JR steel [10] is a non-alloyed structural steel with a minimum yield strength of 235 MPa and a longitudinal Charpy V-notch impact 27 J temperature (T_{27J}) of 20 °C; the typical tensile strength in this material is between 360 and 510 MPa. S460ML [11] represents a thermomechanically rolled weldable fine grain structural steel with a minimum yield strength of 460 MPa and T_{27J}=-50 °C. The tensile strength is usually in the range of 550–720 MPa. Finally, S690 QL [12] is a high yield strength structural steel (>690 MPa) in the quenched and tempered condition with T_{27J}=-40 °C; the typical tensile strength in this material is between 770 and 940 MPa.

For the microstructural analysis of the consequences induced by the flame heat treatment, the material specific Fe-C phase diagram should be considered. For this reason, it is necessary to take into consideration the changes induced by the alloying elements of the three materials analysed on the basic Fe-C diagram. If alloying elements are added to the Fe-C alloy (steel), the position of the A_{C1} and A_{C3} boundaries and the eutectoid composition are modified. The classical diagrams introduced by Bain [13] consider all these effects. It suffices to mention here that: (i) all important alloying elements decrease the eutectoid Carbon content, (ii) Manganese and Nickel decrease A_{c1} and, (iii) Chromium, Silicon and Molybdenum increase A_{c1}. It is possible to estimate the upper and lower critical temperature using the chemical composition of the steel. The following equations [14] provide the approximate critical temperatures for hipoeutectoid steels:

$$A_{C1}(^{\circ}C) = 723 - 20.7\,(\%Mn) - 16.9\,(\%Ni) + 29.1\,(\%Si) - 16.9\,(\%Cr) \quad (1)$$

$$A_{C3}(^{\circ}C) = 910 - 203\,\sqrt{\%C} - 15.2\,(\%Ni) + 44.7\,(\%Si) + 104\,(\%V) + 31.5\,(\%Mo) \quad (2)$$

The accuracy of these formulas, expressed through their standard deviation is ±11.5 °C and ±16.7 °C, respectively. Applying (1) and (2) to the data included in Table 1 yields the following results: S235 JR: T_{AC1}=714 °C; T_{AC3}=846 °C; S460ML: T_{AC1}=704 °C; T_{AC3}=859 °C; S690 QL: T_{AC1}= 706 °C; T_{AC3}=837 °C.

Experimental Techniques

For each steel grade, two plates with geometric dimensions B × W × L=20×500×600 mm^3, manufactured through a rolling process, were available for the research. These plates were heated with a propane torch by applying in all cases a flame pattern in the longitudinal direction, as sketched in Fig. 1.

The devices and parameters of the process were selected in order to reproduce the typical conditions of a flame bending process in a workshop. The first experimental task consisted in a preliminary stage devoted to the training of the technical staff and the calibration of the devices and laboratory apparatus; one of the two available plates for each steel grade was used for these purposes. In this context, the influence of diverse factors involved in the process was analysed allowing the optimum conditions of the procedure to be determined. Thus, it was decided to heat the plates with a propane flame (using a burner nozzle #9 connected to the torch); the flame was applied following a sinusoidal pattern along the strip sketched in Fig. 1. As a general rule, the torch operator heated the plates until the steel glowed cherry red, which indicates a temperature above the upper critical temperature [2].

After that previous stage, the other plate of each material was subjected to the definitive heating, whose influence on the material properties is studied in this research. Each of the plates was instrumented with four thermo-couples (TC_1, TC_2, TC_3 and TC_4) in order to measure the temperatures during the process; these were located in equally distributed holes drilled in the lower surface, in the centre line of the plates, approximately 2 mm below the heated surface (notice that some uncertainty in locating the thermocouples is unavoidable). The average linear velocity of the flame was measured for the three steels yielding 2.5 mm/s (S235 JR), 2.5 mm/s (S460 ML) and 3.7 mm/s (S690 QL), respectively. The thermocouples revealed significant variations of temperature along the heating lines in each plate; the maximum temperatures measured by each of the thermocouples were, the following: S235 JR: TC_1=789 °C; TC_2=827 °C; TC_3=795 °C; TC_4=767 °C. S460ML: TC_1 908 °C; TC_2=882 °C; TC_3=842 °C; TC_4=865 °C. S690QL: TC_1=688 °C; TC_2=671 °C; TC_3=652 °C; TC_4=640 °C. Notice that non-negligible differences among the thermocouples were measured (60 °C for S235 JR, 66 °C for S460ML and 48 °C for S690QL, respectively); this is not surprising as some uncertainties are unavoidable both in the heating process (with the typical possibilities of a workshop) and in the data collection process (for instance, to keep perfectly constant the speed of the flame on the plate, to accurately locate the thermocouples or to ensure the perfect contact between the tip of the thermocouple and the steel). Moreover, the temperatures reached by the S690 steel were lower than for the other two materials; this is a consequence of the higher velocity of the flame in this case (3.7 vs. 2.5 mm/s).

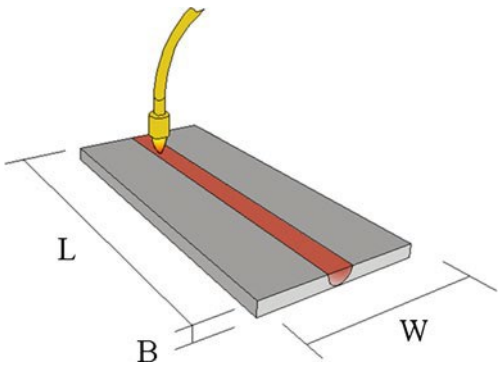

Fig. 1 Sketch of the flame heating pattern applied to the experimental plates

Table 1 Specified chemical composition (% wt.) of the steels analysed in the research [10–12]

Grade	C	Mn	Si	Ni	S	Cr	P
S235JR	≤ 0.17	≤ 1.40	–	–	≤ 0.035	–	≤ 0.035
S460ML	≤ 0.16	≤ 1.70	≤ 0.6	≤ 0.8	≤ 0.02	≤ 0.3	≤ 0.025
S690QL	≤ 0.2	≤ 1.70	≤ 0.80	≤ 2.0	≤ 0.010	≤ 1.5	≤ 0.20

After applying the flame heating to the plates, a set of coupons was taken from different regions (heat affected and non heat affected zones) to analyse several material properties (see details below). Firstly, the chemical composition of each steel was determined by Optical Emission Spectroscopy (OES) in order to confirm the consistency with that specified in [10–12] (see Table 1). The microstructure of the steels was examined through Optical Microscopy (OM) comparing the metallurgical characteristics prior to and after heating. The mechanical behaviour of the material was assessed through the comparison between the results of Vickers hardness tests and tensile tests on the original and treated materials; this same strategy was used to measure the influence of the heating on the fracture properties through Charpy impact tests (together with two additional fracture toughness tests for the S235 JR steel).

Numerical Techniques

In order to accurately determine the evolution of temperature over time in every point of the plates, a Finite Elements model was developed. The simulations were performed with the commercial software ANSYS [15]. The FE simulation consists of a three dimensional (3-D) model of the plate. As only the field of temperatures is relevant for the purposes of the study, a simplified thermal simulation was performed (the stress state was not determined). The SOLID70 element [15] was chosen for meshing the geometry. This element is defined by eight nodes with a single degree of freedom, temperature, at each node. The element is applicable to a 3D, steady state or transient thermal analysis, as in this case. As in previous FE analysis [16–19], the input heat flux of the flame was modelled with a normal Gaussian distribution by considering a moving coordinate system with origin at the centre of the flame circle; the speed of the coordinate system corresponds to the experimental speed of the torch (see above). The surface nodes not directly affected by the flame at each step of the simulation were subjected to airfree convection boundary conditions. The physical and thermal properties of the materials (density, thermal conductivity and specific heat) were available for the research; a generic value for the film coefficient between steel and air was considered.

From this information, it is possible to better interpret the microstructural changes experimentally detected in the materials as a consequence of the flame straightening process. In this sense, the curves relating temperature vs. time at different depths in the plate were determined; hence, the numerical model allows the specific heat treatment applied on any material point in the plates to be obtained.

Experimental Results

This section includes the results obtained in the characterisation of the three steels studied in this research. The analysis of these results, that is, the explanation of the relation between the microstructural characteristics and the experimental results, including the influence of the flame heating, is postponed until the next section.

Chemical Composition

The chemical compositions of the three steels studied are given in Table 2. The comparison between these results and the limits of the material specification [10–12] shows that the chemistry satisfies in all cases what is established there.

Table 2 Chemical composition of the S235JR, S460ML and S690QL steels (% wt.) [10–12]

Grade	C	Mn	Si	Ni	S	Cr	P
S235JR	0.13	0.72	0.20	<0.085	0.016	0.02	0.016
S460ML	0.12	1.57	0.45	<0.085	<0.012	0.04	0.014
S690QL	0.18	1.23	0.29	<0.085	<0.010	0.02	<0.012

Microstructure

The microstructure of the materials was examined through OM. Small coupons were taken from heat affected zones (HAZ) and non HAZ; then, after grinding and polishing up to mirror finish, they were etched with Nital (alcohol and 5 % nitric acid) in order to reveal the microstructure [20]. The details and findings encountered are summarised in the following sections for the grades S235 JR, S460ML and S690QL, respectively

S235 JR steel

In Fig. 2, two macrographs showing the microstructure of the non-heated S235 JR steel at two different depths in the plate (0.5 and 10 mm, respectively) can be appreciated. The microstructure consists of a combination of proeutectoid ferrite (white) and perlite (black), as corresponds to a steel with a 0.13 % Carbon content (see Table 2). The amount of perlite measured in the photographs is approximately 20 %, which is consistent with what may be expected for this steel. In the macrograph taken from the deepest region, Fig. 2(b), the effect of the rolling process to which the plate was subjected is evident; indeed, the ferrite-perlite grains show an elongated shape and a disposition parallel to the surface of the plate.

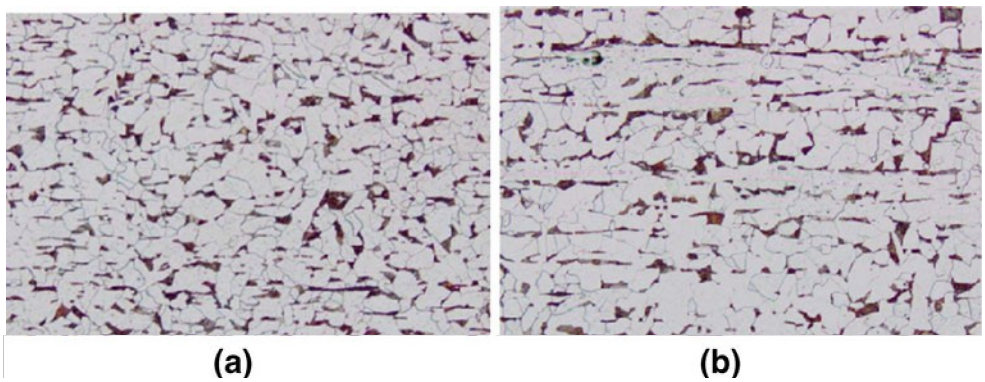

Fig. 2 Macrographs showing the microstructure of the S235 JR steel at two different depths in the plate: (a) 0.5 mm, (b) 10 mm.

In Fig. 3, two macrographs (with different magnification), taken from a depth of 0.5 mm, show the microstructure of the heated S235 JR steel. Two relevant microstructural effects were detected: first, Fig. 3(a), the grain has experienced a noticeable refinement: prior to heating the average size (expressed through the equivalent diameter) of the grains was 20±4 μm whereas after that, it decreased to 14±4 μm. Second, cementite precipitates are appreciated in some grain boundaries, see Fig. 3(b) (some arrows are included in the photograph to facilitate the inspection). This type of cementite is known as "tertiary cementite" and is usually considered to be responsible for the embrittlement of low carbon steels [21, 22].

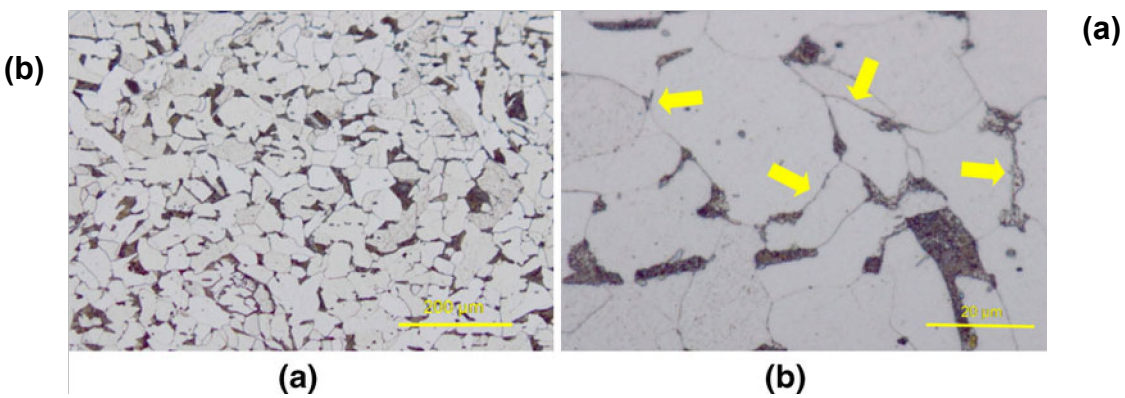

Fig. 3 Macrographs showing the microstructure of the heated S235 JR steel at an approximate depth of 0.5 mm

S460 ML steel

In Fig. 4, two macrographs (with different magnification), taken from a depth of 0.5 mm, show the microstructure of the non-heated S460 ML steel. A combination of proeutectoid ferrite (white) and perlite (black) can be clearly seen, which is coherent with what is expected for a 0.12 % Carbon content steel (see Table 2). In this case, the elongated non-symmetrical disposition of grains created by the rolling process is evident even in this near-to-surface macrograph. The presence of this rolling pattern was confirmed all throughout the thickness of the plate (20 mm), being slightly more intense in its core (approximately between 8 and 12 mm deep). The macrograph in Fig. 4(b) shows another interesting feature consisting in the large scattering in the shape and size that can be appreciated in the ferrite grains.

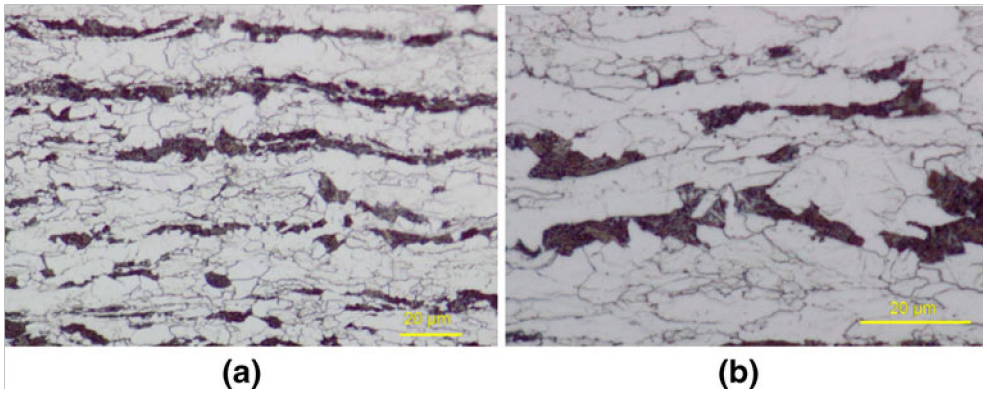

Fig. 4 Macrographs showing the microstructure of the nonheated S460ML steel at an approximate depth of 0.5 mm

Concerning the microstructure of the flame treated S460 ML steel, a micrograph obtained at a depth of about 0.5 mm is shown in Fig. 5. The alteration of the morphology of the grains is highlighted in this photograph: both the size and shape of the grains have changed and the needle-shaped (acicular) grains present prior to heating have disappeared; moreover, larger non uniformity is present in the grain size distribution. These features are a consequence of the recrystallization induced by the flame heating process, which is particularly intense on the surface of the plate (these features were observed even at depths of 10–12 mm from the surface of the plate).

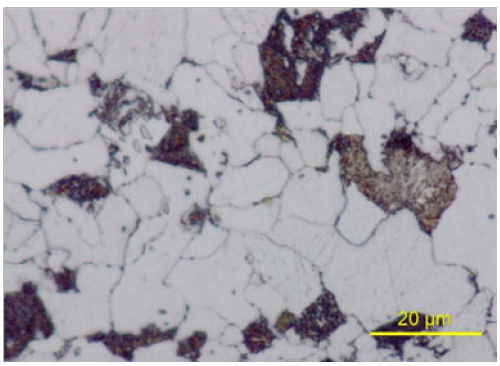

Fig. 5 Macrograph showing the microstructure of the heated S460ML steel at an approximate depth of 0.5 mm

S690 QL steel

The microstructure of the non-heated S690 QL steel can be seen in Fig. 6 (this macrograph was taken at a depth of 15 mm). It is worth noting that no relevant changes in microstructure were observed throughout the thickness of the plate. A combination of bainite and ferrite constitutes the microstructure of this material, in accordance with what is

expected (see above). Although the maximum temperature reached during the heating in this case is only 688 °C, several relevant microstructural changes were induced by the process. In general, the material has undergone a second tempering, superimposed on the original one. This effect is clearly appreciated in the upper part of the plate, particularly at a depth less than 5 mm. Figure 7(a), which is taken at a depth of 0.5 mm, reveals the complete nodulization of the carbides, originally distributed through the bainitic pattern. This effect decreases with depth but, even at 5 mm, see Fig. 7(b), the carbides show a slight tendency to group into clusters. No modification in the grain size or shape is appreciated, which is consistent with the fact that the maximum temperature is below T_{Ac1}.

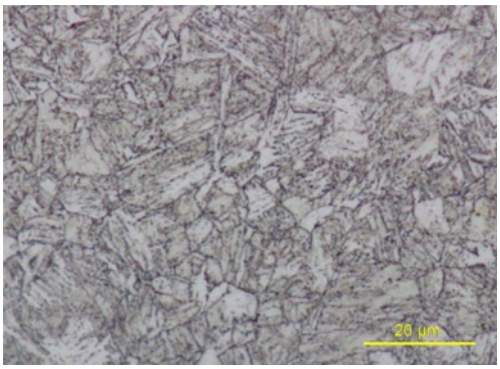

Fig. 6 Macrograph showing the microstructure of the non-heated S690QL steel at an approximate depth of 15 mm are below the limits established or recommended (see Table 4).

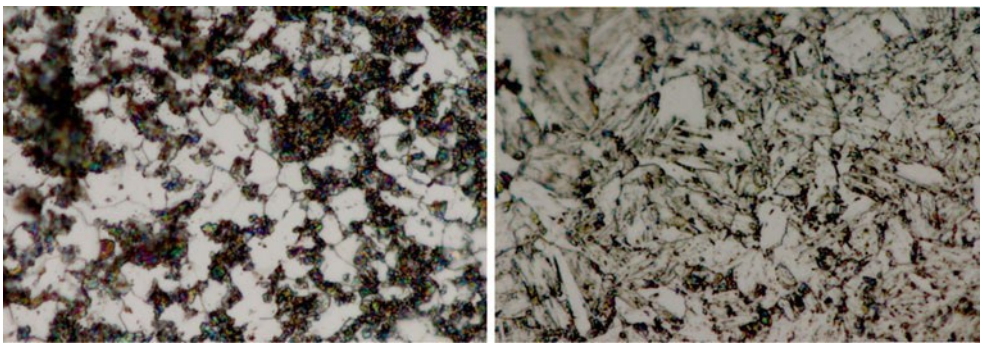

Fig. 7 Macrograph showing the microstructure of the heated S690QL steel at an approximate depth of: (a) 15 mm, (b) 5 mm.

Mechanical Characterisation

Vickers hardness tests

Vickers hardness tests (1 kgf, 20 s.) were performed on each of the grades and material conditions. The tests were performed across the thickness of the specimen below the surface heated by the flame (see Fig. 8). The results are represented in Fig. 9 and summarised in Table 3 where the average values and the standard deviation obtained in each case are included. Several interesting features can be appreciated:

- The intrinsic differences between the three materials are clearly highlighted: the hardness of the S690QL is noticeably higher than that of the S460ML, this material being, in turn, harder than S235 JR.

- S235 JR did not undergo any substantial change in hardness; on the other hand, both S460ML and S690 QL steels became softer as a consequence of the heat treatment experienced. On average, the Vickers hardness decrease in these materials is up to 13 % and 26 %, respectively, see Table 3.

- The hardness of the three steels prior to heating shows only slight variations through the thickness, as expected for materials which are supposed to be homogeneous; this statement is also true for S235 JR after heating. Nevertheless, a slight variation in hardness can be seen for S460ML and S690QL steels: in both cases the material becomes softer in the proximity of the surface heated, approximately up to a depth of 10 mm.

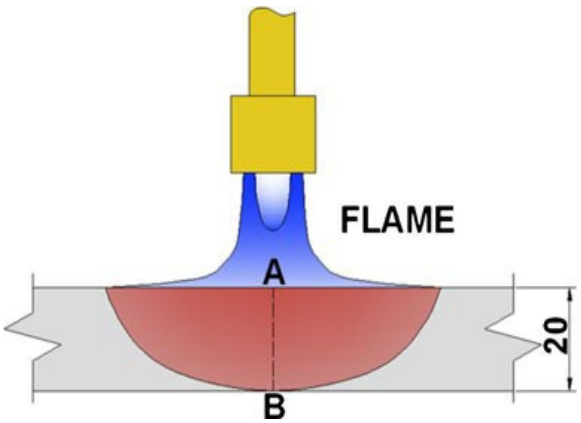

Fig. 8 Sketch showing the region (line AB) where the Vickers tests were performed.

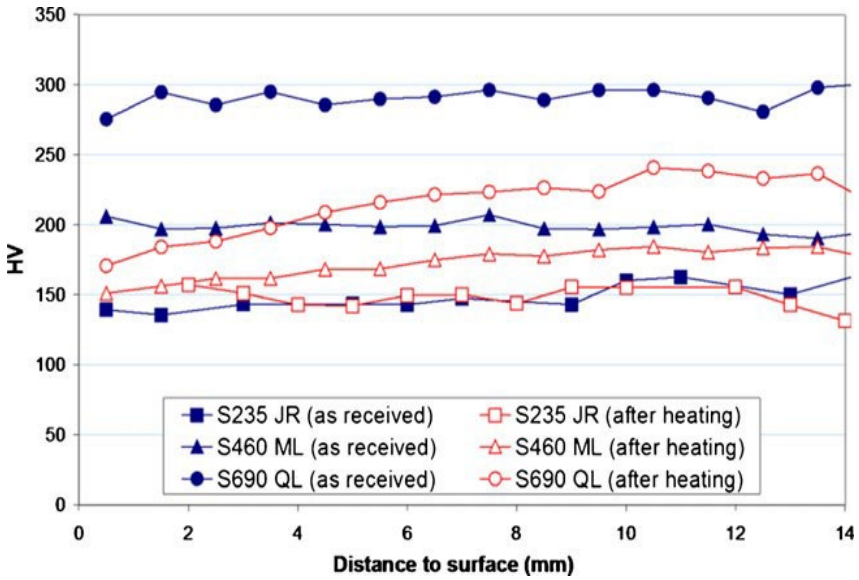

Fig. 9 Results of the Vickers tests performed through the thickness of the plates, prior to and after heating, for each steel grade

Table 3 Summary of the results of the Vickers hardness tests

Material	As received	After heating	Variation (%)
S235 JR	147±6	147±11	0
S460 ML	198±4	172±11	−13
S690 QL	291±7	215±21	−26

Tensile tests

The experimental scope of this investigation included some tensile tests to be performed both under as-received (AR) after heating (AH) conditions. In Fig. 10, the location of the specimens in the plates and their geometrical dimensions are shown. The design of the specimens as well as the parameters of the tests were selected following the stipulations of the ASTM Standard [23]. The layout sketched in Fig. 10 indicates that the tensile tests are representative of the average mechanical behaviour of the material approximately 10 mm in depth from the surface of the plate. One nonheated specimen plus one HAZ specimen were obtained for each material.

The tests were performed at room temperature (~20 °C). The load vs. elongation curves were recorded up to fracture from them, the stress vs. strain (engineering variables) curves, represented in Fig. 11, were calculated; the main mechanical parameters (proof yield stress, $s_{Y(0.2\%)}$, tensile strength, s_U and strain at fracture, e_U) are summarised in Table 4. The most relevant aspects that can be gathered from the curves are next summarised:

- The intrinsic mechanical differences between the materials are evident. S690 QL is noticeably more resistant than S460ML, this being, in turn, more resistant than S235 JR. This result is in accordance with what may be expected and with the results of the Vickers hardness tests. As can be observed in Table 4, the three materials (as received condition) satisfy the requirements and recommended values of yield stress and tensile strength mentioned above.

- The curves clearly show that the influence of the flame heating on the mechanical response is strongly material dependent: following the same tendencies that were appreciated in the previous section, the flame treatment hardly modifies the properties of S235 JR steel, whereas the change in the other materials varies from moderate (S460ML) to noticeable (S690QL). Indeed, the yield stress in both materials and tensile strength of S690QL

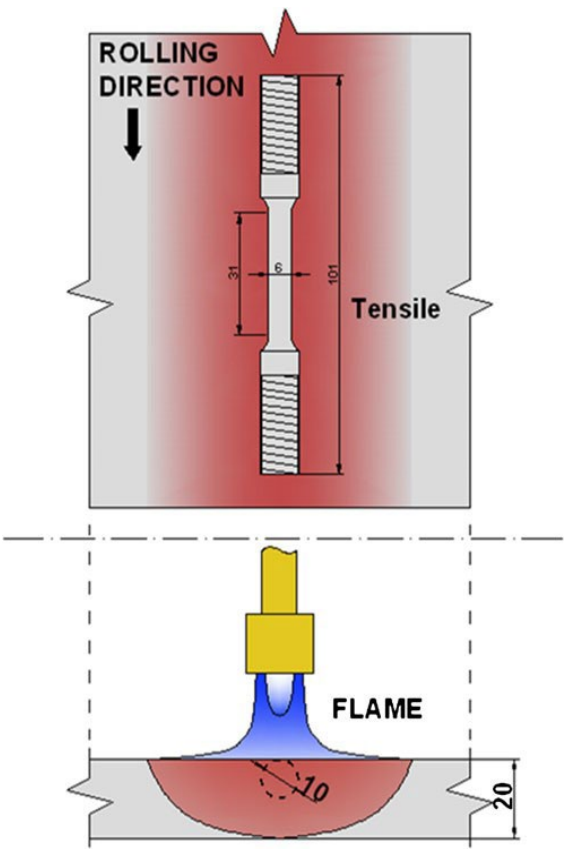

Fig. 10 Sketch showing the disposition of the tensile specimens in the plates

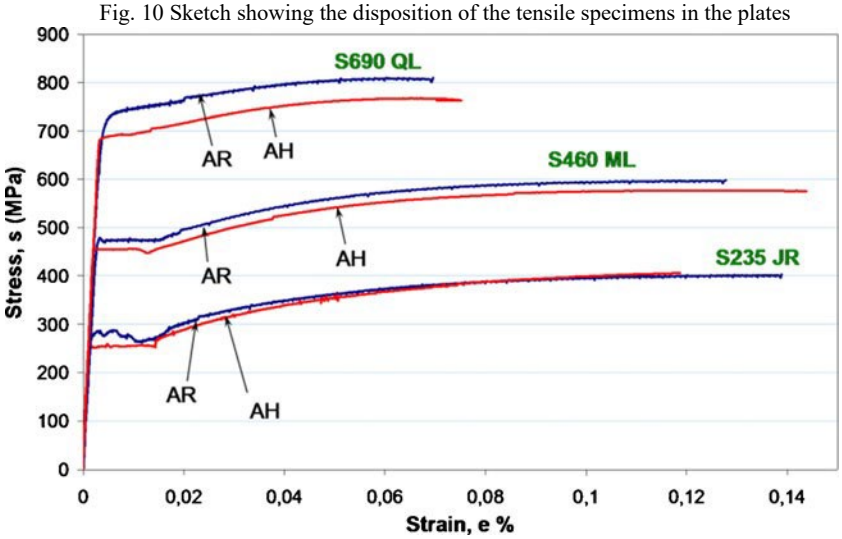

Fig. 11 Stress vs. strain curves (as received and flame heated condition).

Table 4 Summary of the relevant results obtained in the tensile tests

Material	Property	As received	After heating	Variation (%)
S235 JR	$s_{Y\ (0.2\%)}$ (MPa)	284	247	−13.0
	s_U (MPa)	402	410	2.0
	e_U (%)	13.8	11.8	−14.5
S460 ML	$s_{Y\ (0.2\%)}$ (MPa)	469	455	−3.0
	s_U (MPa)	597	576	−3.5
	e_U (%)	12.7	14.4	13.4
S690 QL	$s_{Y\ (0.2\%)}$ (MPa)	732	688	−6.0
	s_U (MPa)	809	767	−5.2
	e_U (%)	6.9	7.5	8.7

Fracture Characterisation

A set of Charpy V notch (CVN) specimens was obtained for each material and heat treatment condition; the number of as-received tested specimens for each material was between 11 and 12 whereas this number for flame treated specimens was between 5 and 6. The geometric characteristics, the fabrication and the testing of the specimens were conducted following the requirements of [24]. The sketch in Fig. 12 shows the location and orientation of the specimens: according to this, they are representative of the average fracture behaviour of the material approximately 10 mm in depth from the surface of the plate.

The purpose of this experiment is to characterise the fracture response (through CVN impact tests) as a function of temperature, that is, to obtain the material CVN curves. The temperature range was selected in order to include, when possible, the lower shelf, the ductile-to-brittle transition region and the upper shelf. The experimental results, expressed in terms of the absorbed energy vs. test temperature, are included in Fig. 13 (S235 JR), Fig. 14 (S460ML) and Fig. 15 (S690QL). To facilitate the subsequent analysis, the CVN curves were fitted to the hyperbolic tangent curve shown in Eq. (3) (as recommended in [24]):

$$E = A + B\,Tanh\left(\frac{T - C}{D}\right) \tag{3}$$

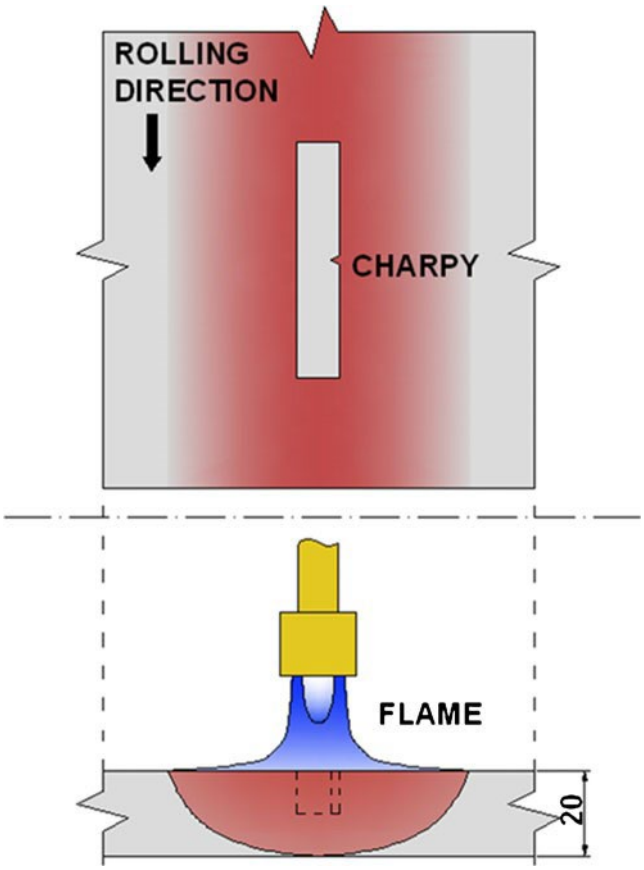

Fig. 12 Sketch showing the disposition of the CVN specimens in the plates

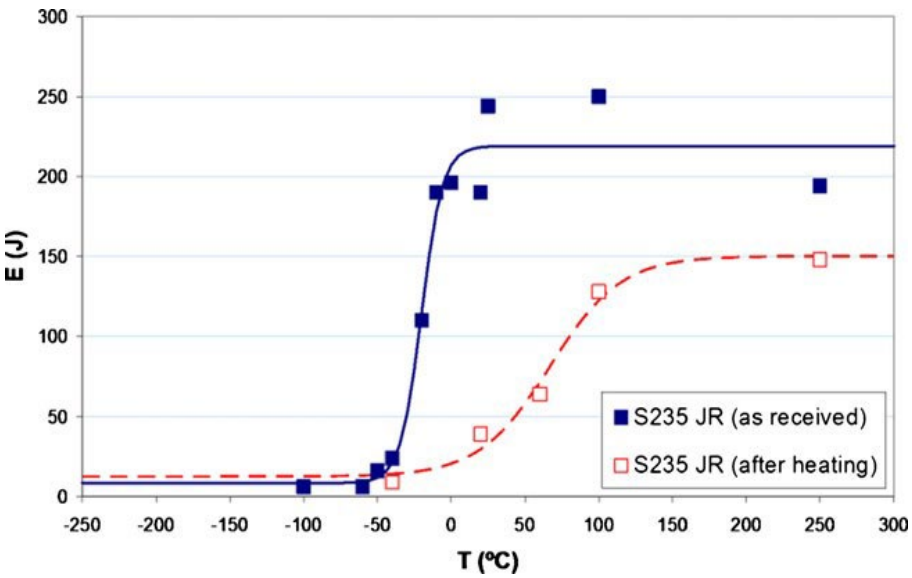

Fig. 13 CVN curves (energy vs. temperature) for S235 JR steel (as received and after heating condition

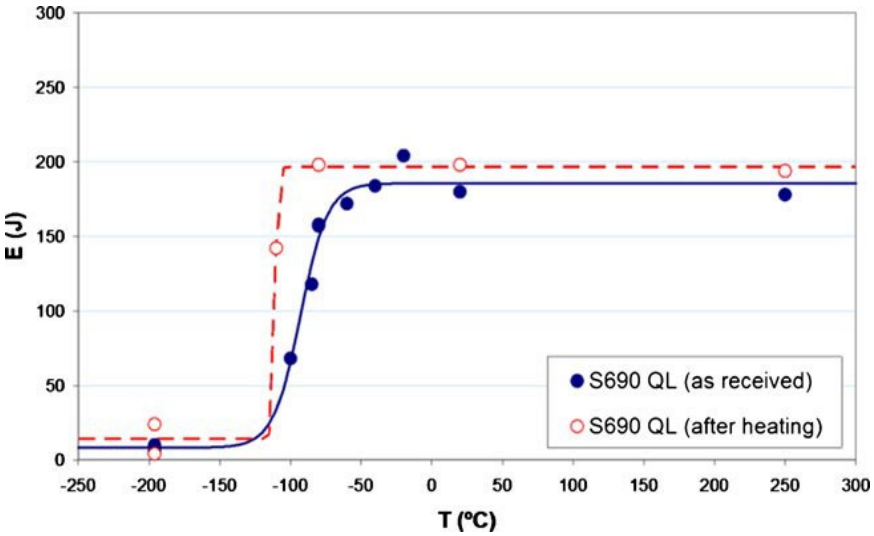

Fig. 14 CVN curves (energy vs. temperature) for S460ML steel (as received and after heating condition

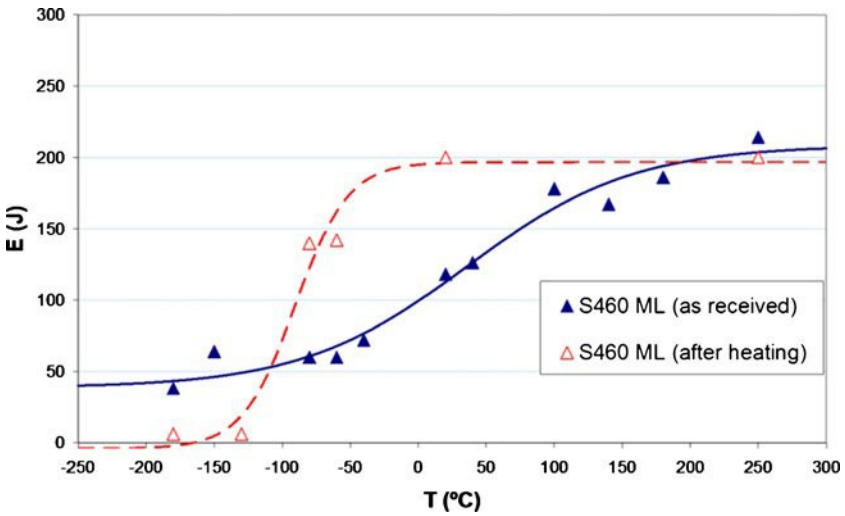

Fig. 15 CVN curves (energy vs. temperature) for S690 QL steel (as received and after heating condition

In this expression, A, B, C and D are free parameters to be obtained through a least squares fitting procedure of the experimental data (energy, E, vs. temperature, T). From them, the values of the upper shelf energy, USE (which is equal to the sum of the parameters A and B), the transition temperature represented by the parameter C, the width of the transition region, described through the parameter D, and the transition temperature T_{27J}, were determined for the three materials, both under as-received and after heating conditions. All these results are collected in Table 5.

The curves included in Figs. 13, 14 and 15 clearly show that the influence of the flame heating on the fracture response is, again, strongly material dependent. The S235 JR steel has undergone a marked embrittlement as a consequence of the flame heating. As can be seen in Fig. 13 and Table 5, the USE decreased from 219 J to 150 J, this phenomenon being accompanied by an increase in T_{27J} from -37.1 °C to 15.5 °C (it is worth noting that a value of T_{27J}= 20 °C is demanded for this material). The influence of the flame on the S460ML steel is certainly more complex (see Fig. 14) as a complete modification in the shape of the curve occurred; in this sense, the material embrittled in the lower shelf region whereas the

fracture response in the transition region clearly improved: the transition temperature C changed from 35.7 °C to -90.4 °C (T_{27J} could not be determined in the as-received condition); moreover, the USE was scarcely affected by the treatment (206 J vs. 197 J). In both cases the requirement of T_{27J}=-50 °C is fully satisfied. Finally, the fracture behaviour of the S690QL grade hardly modified as a consequence of the flame heating process; specifically, the transition temperature T_{27J} changed from -113.4 °C to -113.5 °C (the requirement for this material being T_{27J}=-40 °C) and the USE from 186 J to 197 J. Only slight differences are appreciated in the upper part of the transition region but they could be motivated by the intrinsic scattering of the fracture in this range of temperatures.

Table 5 Relevant results obtained from the Charpy characterisation

Material	Property	As received	After heating	Variation
S235 JR	USE (J)	219	150	−69
	C (°C)	−20.3	66.9	87.2
	D (°C)	−14.4	48.1	62.5
	T_{27J}	−37.1	15.5	52.6
S460 ML	USE (J)	206	197	−9
	C (°C)	35.7	−90.4	−126.1
	D (°C)	122.0	38.7	−83.3
	T_{27J}	–	−123.1	
S690 QL	USE (J)	186	197	11
	C (°C)	−93.0	−110.9	−17.9
	D (°C)	19.1	2.0	−17.1
	T_{27J}	−113.4	−113.5	−0.1

After performing the Charpy tests, the broken surfaces were carefully examined through OM in order to identify the mechanisms that lead to the fracture, as well as how they evolved with temperature. Some representative macrographs can be appreciated in Fig. 16 (S235 JR), Fig. 17 (S460ML) and Fig. 18 (S690QL). The photographs were selected to represent, for each material and condition, the fracture appearance in the lower shelf, the transition region and the upper shelf. As can be seen, for low temperatures the specimens hardly show any plastic deformation, the fracture surfaces being flat and brilliant. As temperature rises, a noticeable plastic deformation took place during fracture thus leading to a large amount of lateral expansion and a fibrous appearance of the fracture surfaces; these features are evident in the photographs corresponding to the transition region and, in particular, in those obtained from specimens which were tested in the upper shelf regime. The fracture appearance of the broken specimens fabricated with the S460ML steel deserves a specific commentary: as can be seen in Fig. 17, the influence of the rolling to which the plate was subjected is evident in the fracture surfaces, in particular in those tests corresponding to the lower shelf and the transition region. The influence of the rolling of the plate is of minor importance at higher temperatures, as becomes evident when comparing macrographs Fig. 17(c) and (f) (as-received material tested at 140 °C and flame heated material tested at 250 °C, respectively). The comparison between macrographs Fig. 17(a) and (d) (as received material tested at 150 °C and flame heated material tested at -135 °C, respectively) allows the differences in plastic deformation between these specimens to be observed: the former shows some amount of lateral expansion whereas this feature is completely absent in the latter. This characteristic is coherent with the behaviour of the material in the lower shelf region, see Fig. 14.

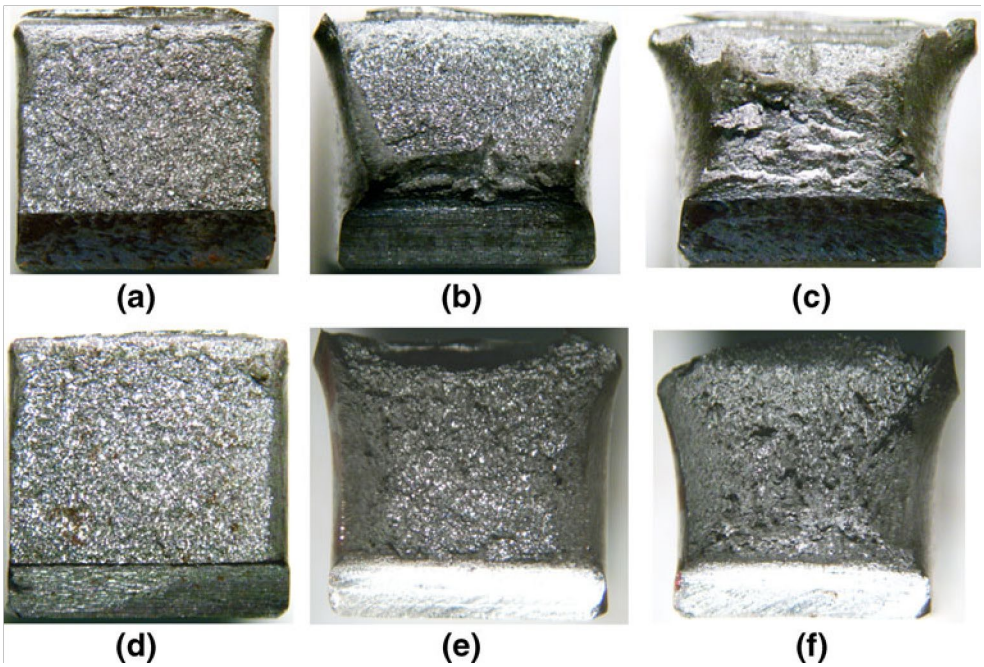

Fig. 16 Macrographs showing the fracture surfaces of the S235 JR CVN specimens. As received condition: (a) −50 °C, (b) 20 °C, (c) 250 °C. Flame heated condition: (d) −40 °C, (e) 60 °C, f 100 °C

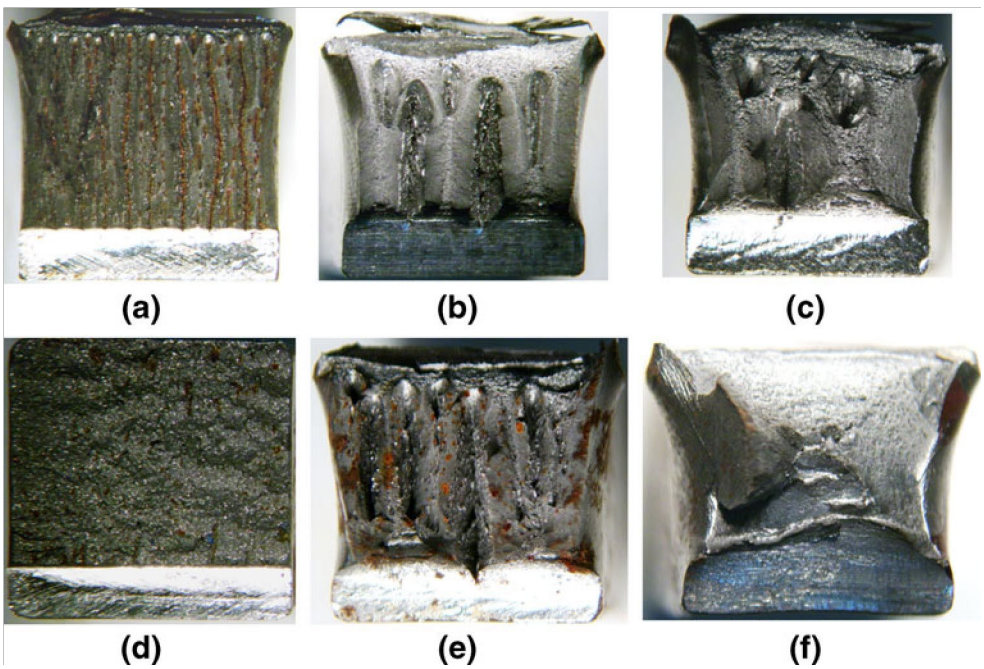

Fig. 17 Macrographs showing the fracture surfaces of the S460 ML CVN specimens. As received condition: (a) −150 °C, (b) 40 °C, (c) 140 °C. Flame heated condition: (d) −135 °C, (e) −60 °C, (f) 250 °C

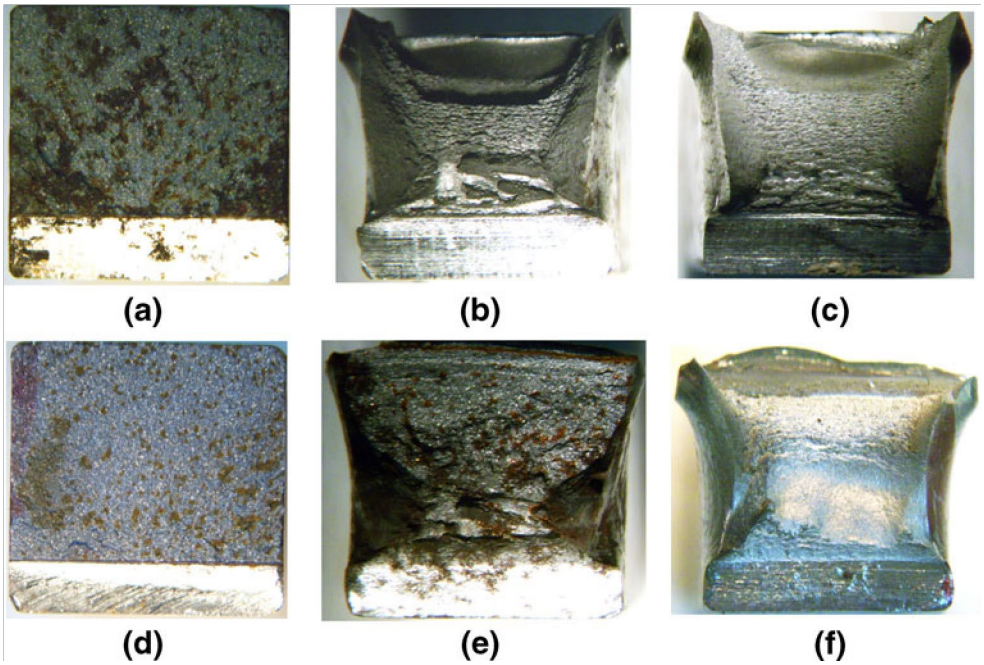

Fig. 18 Macrographs showing the fracture surfaces of the S690 QL CVN specimens. As received condition: (a) −196 °C, (b) −60 °C, (c) 20 °C. Flame heated condition: (d) −196 °C, (e) −110 °C, (f) 250 °C

Extended characterisation of the S235 JR steel

As stated in the previous section, the S235 JR steel has undergone a noticeable embrittlement as a consequence of the flame heating. This conclusion can be solidly established -at least in a semi-quantitative way- from the examination of Fig. 13. Nevertheless, although the CVN curves are useful to highlight general features related with the material′s fracture resistance, it is a limited tool for structural purposes. As demonstrated in the field of Fracture Mechanics [25, 26], the J-integral concept, originally proposed by Rice [27], represents the proper material parameter to describe the fracture toughness when material plasticity is present during fracture. The J-Δa curve of a material represents its resistance to stable crack growth ("a" being the crack length and Δa its extension due to the applied loads) when ElasticPlastic Fracture Mechanics (EPFM) conditions are present during propagation. For this purpose, definition (4) for the Jintegral as an energy release rate [25, 26] has been used in this research. Thus, J is a measure of the energy available for a virtual (small) crack extension, δa. It is defined [25, 26] as the virtual change of potential energy (δπ) in a deformed body due to the virtual enlargement of the crack area (δA, where δA=B·δa, B the thickness of the specimen). The potential energy, π, is defined as the difference between the strain energy stored in the body, U, and the work done by the external forces, F; therefore:

$$J = \frac{\delta \Pi}{\delta A} = \frac{1}{B}\frac{\delta \Pi}{\delta a} \qquad (4)$$

The definition of the specimens, the experimental details and the interpretation of the results were established following the criteria of the ASTM standard [28]. In this sense, two S235JR CVN specimens (one in the as-received condition and the other in the flame treated condition) were precracked through fatigue (to induce the presence of an initial sharp crack, a0) and subsequently tested at room temperature in three-point bending. The crack extension during the test was determined using the so-called elastic compliance technique (which is advantageous when only one single specimen is available, see [25, 26, 28] for details). Finally, the fracture resistance curves, which are represented in Fig. 19, were obtained. Following

what is recommended in [28], the experimental points (Δa, J) were fitted though a least squares procedure to the power law form (5) (thus determining the parameters C1 and C2): the fittings are included in Fig. 19.

$$J = C_1 (\Delta a)^{C_2} \qquad (5)$$

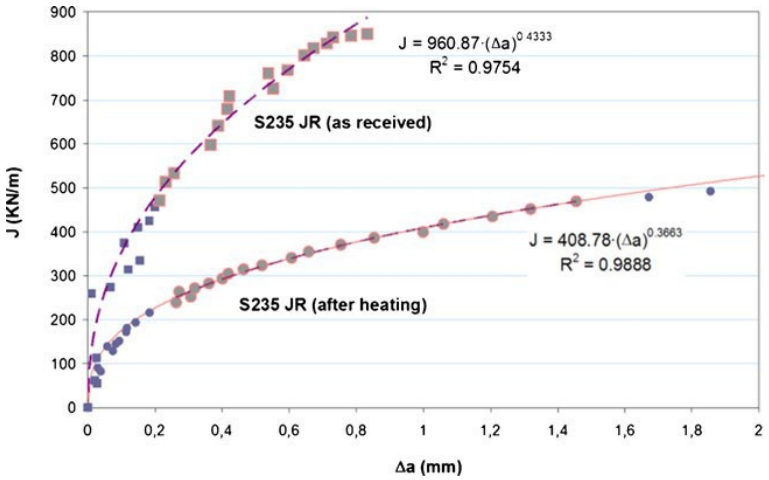

Fig. 19 Fracture resistance curves (J-integral vs. crack extension, Δa) obtained for the S235 JR steel comparing the as received response with the flame treated behaviour.

The curves highlight the significant difference in fracture response between the original and the heat treated S235 JR material. The original material shows a noticeable toughness and a rising resistance curve. This behaviour is of great impor tance from the structural point of view because, if a crack grows a small amount in this material when a stress state is applied, it cannot grow further unless the stress increases. On the other hand, the flame treated material has undergone a significant embrittlement which influenced not only the absolute values of toughness but the general shape of the curve: indeed, the slope of the curve substantially decreased as highlighted through the comparison of the parameter C_2.

Validation of the FE Model

Figure 20 shows the curves determined numerically relating temperature vs. time as a function of the depth in the plate. Figure 20(a) was obtained imposing a velocity of the torch of 2.5 mm/s (S235 JR and S460ML steels) whereas Fig. 20 (b) corresponds to a velocity of 3.7 mm/s (S690QL steel).

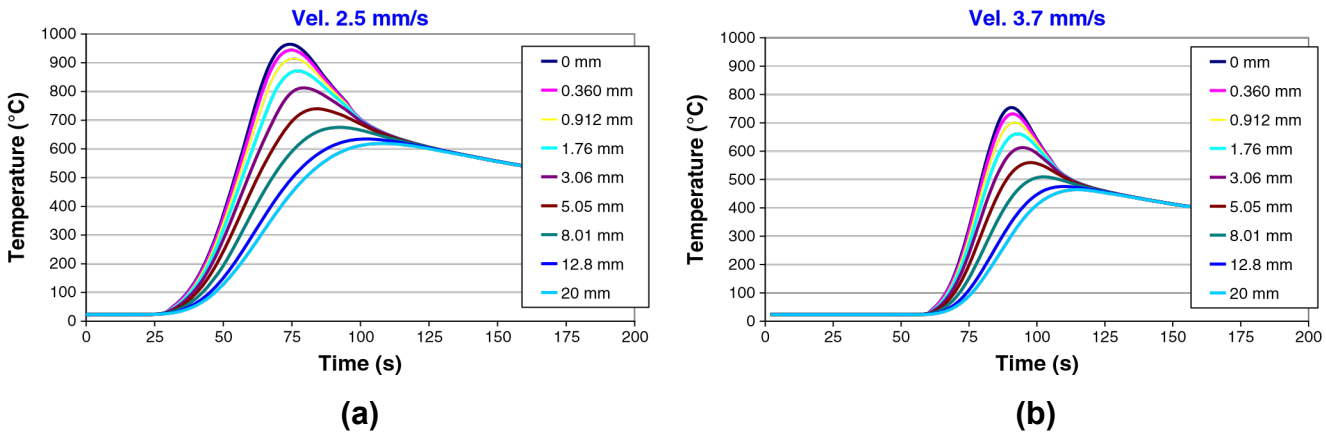

Fig. 20 Finite Elements temperature vs. time curves as a function of the depth in the plate. (a) 2.5 mm/s (S235 JR and S460ML steels); (b) 3.7 mm/s (S690 QL steel)

The graphs included in Fig. 21 demonstrate the reliability of the FE model. For instance, Fig. 21(a) compares the temperature vs. time curves determined numerically; for this purpose, the experimental data recorded by the four thermocouples in S235 JR steel were superimposed on Fig. 20(a) (2.5 mm/s); as can be seen, the agreement between the curves is truly satisfactory. In addition, the curves relating the maximum temperature reached, T_{max}, as a function of the speed of the torch for each depth in the plate are represented in Fig. 21(b). Notice that the experimental results of maximum temperature, also included in the figure, lie approximately between the curves corresponding to a depth of 0.912 mm and 3.06 mm, close to the curve corresponding to a depth of 2 mm (which is the approximate depth of the thermocouples in the plate). Notice as well that, as mentioned above, the experimental uncertainties are non-negligible, Again, the numerical predictions provide a reliable result.

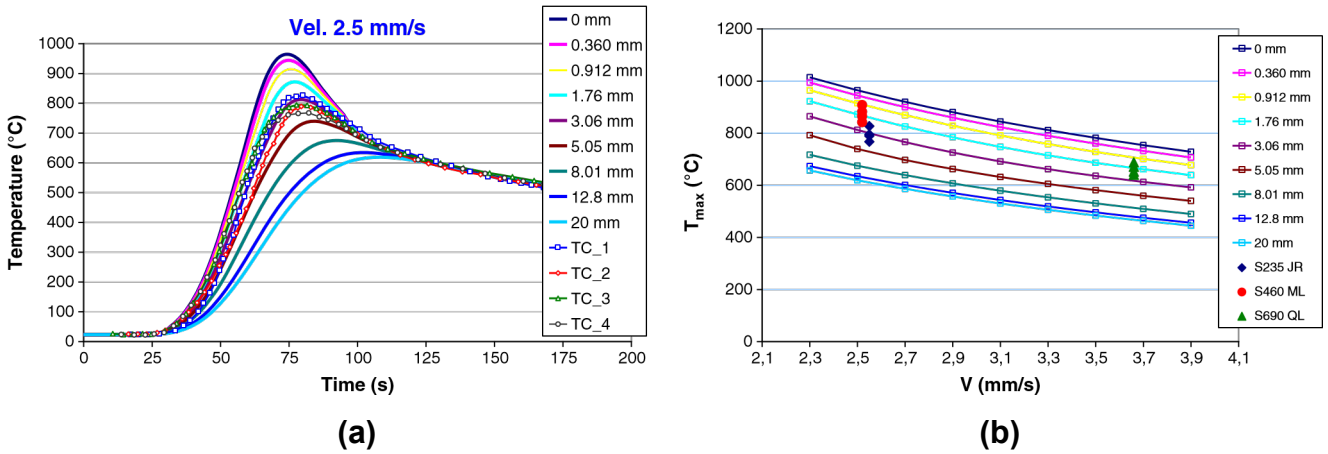

Fig. 21 (a) Comparison between the temperature vs. time curves determined numerically and experimentally (S235 JR steel, 2.5 mm/s); (b) curves relating the maximum temperature, T_{max}, as a function of the speed of the torch for each depth in the plate; the experimental results of maximum temperature are included in the figure

Analysis and Discussion of the Experimental Results

It is a well proven matter of fact that the mechanical properties of the materials are the consequence of their microstructural nature. In this sense, from the empirical study carried out in this research, it was possible to determine the role played by the microstructure, as well as its variation due to the thermal treatment, on the mechanical (Vickers, tensile) and fracture (CVN, J-Δa) properties of the three steels analysed.

S235 JR Steel

During the flame heating process, the S235JR steel undergoes a series of different thermal cycles in function of the distance to the heating surface. As shown by the FE, Fig. 20 (a), this material remains at a temperature higher than ~750 °C (T_{AC1}=714 °C; T_{AC3}=846 °C) for at least 10 s in the 3 mm band closest to the surface. This process, which may be considered as an "intercritical annealing", causes the partial dissolution of pearlite which, in turn, as a result of the subsequent cooling, may lose its laminar (banded) structure (Fig. 3 (a)) previously appreciated in the original microstructure (Fig. 2(a)).

A second appreciable aspect is caused by the high temperature reached, exceeding T_{AC3}=846 °C, by the material in the 2 mm band nearest the surface. This process results in the transformation of the existing phases in austenite, this phenomenon being known as a "full annealing". The annealing of low and medium carbon steels is achieved by heating above the transformation temperature, that is above T_{AC3}. In this range of temperatures, the transformation from alpha-iron to gamma-iron, as well as the formation of a large number of small austenite grains, take place regardless of the original size of the grains of ferrite or pearlite [29]. Both features can be observed in Fig. 3(a). Moreover, the possibility of the formation of martensite and / or bainite if temperatures above T_{AC1}=714 °C are reached should be considered; in this case, the austenite

that precipitates in the ferrite grain boundary if the subsequent cooling is very fast will result in martensite islands surrounded by a matrix of ferrite as in the 'dual-phase' steels.

A third point to notice here is the formation of "tertiary cementite" as a result of the cooling conditions to which the material is subjected. As shown by the FE model, see Fig. 20(a), the cooling rate below 600 °C is very slow at any depth, thus enabling the formation of such a microstructure; indeed, the time for the temperature to decrease from 600 °C to 400 °C is substantially longer than 100 s. This feature is shown in Fig. 3(b). Previous research has shown that the tertiary cementite promotes the embrittlement of steels [21, 29], as in this case.

The mechanical characterisation is based on the Vickers and tensile tests. As a general feature, no noticeable changes in mechanical behaviour can be attributed to the flame heating process. The profile of Vickers tests represented in Fig. 9 shows only a slight variation in hardness with the depth of the plate, both in the as-received and the heat treated conditions; moreover, no relevant differences are appreciated between them. This implies that the effect of the rolling process highlighted by the microstructural study does not influence the Vickers test results. Moreover, the grain refinement that took place as a consequence of the flame treatment did not have any relevant effect on the material hardness. The results obtained in the context of the tensile characterisation are in good agreement with what is stated above. Only a slight change in the yield stress was detected but, as can be observed in Fig. 11, the irregular shape of the yield plateau recommends that caution should be taken with this conclusion. Moreover, the differences in tensile strength or strain at fracture are completely negligible. Concerning the fracture behaviour, Figs. 13 and 19 demonstrate that a large embrittlement occurred as a consequence of the flame treatment. This can only be attributed to the cementite precipitation appreciated in some grain boundaries, see Fig. 3(b). As stated above, this tertiary cementite is considered to be responsible for the embrittlement of low carbon steels [22, 29], as in this case.

S460 ML Steel

As demonstrated above, this steel shows a strongly deformed microstructure because of the rolling process, Fig. 4(a). Moreover, large scattering in the shape and size of the ferrite grains is shown in Fig. 4(b). This is a typical consequence of a controlled hot rolling process: the first part of the rolling takes place when the material is in the austenitic condition (thus inducing recrystallizations that give place to rounded and similar sized grains) whereas the final part is developed in the ferrite-austenite region of the phase diagram so that recrystallization occurs on deformed ferrite grains [21, 22].

This type of deformed structures are highly reversible if a heating process able to reorder the microstructure into a new more stable one is applied (compare Figs. 4 (b) and 5). The consequences of the heating experienced by the steel depend on the temperature reached. As the upper surface band of the plate exceeded the temperature T_{Ac1}= 704 °C, the material was subjected to an intercritical or full annealing treatment, depending on whether the steel reached the temperature T_{Ac3}=859 °C. These two treatments lead the formation of austenite as well as the recrystallization of ferrite, Fig. 5. The pictures collected in Fig. 22 allow these aspects to be appreciated; thus, in Fig. 22(a), taken at a depth of 0.5 mm, the grain coarsening because of the full annealing treatment received by the material can be seen. Moreover, Fig. 22(b), taken at a depth of 7.5 mm, shows the recrystallization without the grain coarsening characteristic of the intercritical annealing treatment.

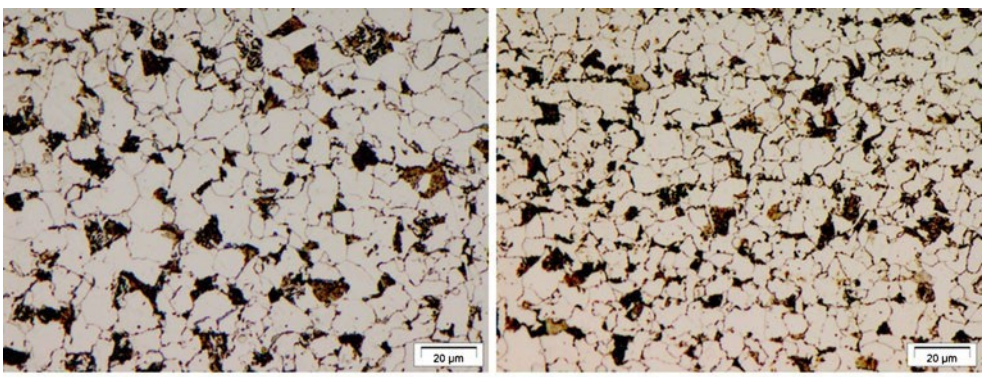

Fig. 22 Macrographs showing the microstructure of the heated S460 ML steel at an approximate depth of: (a) 0.5 mm, (b) 7.5 mm

The complete process undergone by the material as a consequence of the thermal cycle is characterised by several stages: first, a recovery period occurs; during this process ductility increases and strength slightly decreases. When the next stage of recrystallization occurs, equiaxed grains are formed from elongated grains. Finally, a prolonged time at a certain temperature allows some of the newly formed grains to grow at the expense of other grains. During this stage, strength decreases and ductility increases significantly.

The profile of Vickers tests in Fig. 9 shows that there is no noticeable change in hardness with the depth in the as-received condition. This is consistent with the microstructural analysis where no relevant variations were detected. The heated material, in turn, shows a tendency to a softer behaviour in the proximity of the surface; this can be explained as a consequence of the recrystallization induced by the flame heating process which is particularly intense on the surface of the plate: indeed, as stated above, the size and shape of the grains have changed and the acicular grains present prior to heating have disappeared. The consequences of the recrystallization also become evident when comparing the tensile response of the material in the as-received condition and after heating: a general loss in mechanical resistance together with a slight increase in ductility occurred, as can be appreciated in Fig. 11. These features are reflected in the fracture response of the material, as can be seen in Fig. 14, when an improvement in fracture toughness is evident in the treated material as compared with the original condition.

S690 QL Steel

As indicated above, the speed of the torch in this case was significantly higher than the other steels. This fact results in a lower maximum temperature and different cooling patterns. The analysis represented in Fig. 20(b) states that, as no point in the plate has reached the temperature A_{C1}, this martensitic-bainitic material was subjected to a tempering heat treatment. The tempering is more pronounced near the heated surface and decreases with the depth. Figure 7 provides a comparison between two points located, respectively, in the vicinity of the heated surface, at a depth of 0.5 mm (Fig. 7(a)) and 5 mm deep (Fig. 7(b)). In the first case, the transformation of the typical structure of carbides in plates or sheets into nodular clusters can be seen. However, in the second one, only the partial solution of such carbides is shown.

Figure 9 shows that this material has undergone an intense change in hardness due to the flame heating. This variation is particularly intense in the proximity of the surface of the plate (where the hardness reduces from 275.5 to 170.5) and less pronounced in depth. This has its corresponding counterpart in the tensile characterisation: both the yield stress and the ultimate strength reduced noticeably. This behaviour is perfectly reasonable in view of the second tempering detected in the microstructural

Summary and Conclusions

In this research, the consequences of applying a flame straightening procedure by means of a propane torch on three different structural steels (S235 JR, S460ML and S690QL) were analysed. The results of the microstructural study performed through optical microscopy, comparing the microstructural features present on each of the three materials prior to and after receiving the flame heat treatment, were correlated with the mechanical behaviour (assessed through micro-hardness Vickers and tensile tests) and with the fracture resistance (determined through impact Charpy tests and, in the case of the S235 JR steel, two J-integral fracture toughness tests). This study revealed very different behaviours, depending on the material, as summarised next:

- Concerning the S235 JR material, the grain has undergone a noticeable coarsening as a consequence of the flame treatment. Moreover, tertiary cementite precipitates were appreciated in some grain boundaries. Neither the hardness of this material nor its tensile response were modified by the flame straightening; nevertheless, a large embrittlement occurred, which is attributed to the precipitation of the tertiary cementite mentioned above.

- The size and shape of the grains of the S460ML steel were noticeably affected as a consequence of the recrystallization induced by the flame heating. This microstructural change moderately modified the mechanical behaviour of the material both from the point of view of the Vickers micro-hardness as well as the tensile tests (the yield stress of the heated materials is only 455 MPa, which is slightly below the material's nominal yield stress of 460 MPa). Moreover, a complete modification in the shape of the CVN curve took place.

- The S690 QL material has undergone a second tempering, superimposed on the original one, due to the flame heat treatment. The Vickers micro-hardness and the tensile tests show that a noticeable change in mechanical properties occurred; indeed, the yield stress and tensile strength are clearly below those demanded for this material. This is of particular relevance, as the maximum temperature reached during the flame straightening was only 688 °C. Finally, the fracture behaviour of the S690 QL grade hardly modified as a consequence of the flame heating process.

As can be appreciated, the influence of the flame straightening procedure on the microstructure, mechanical or fracture behaviour clearly depends on the nature of the steel receiving this sort of heat treatment. These results provide clear evidence that it is not possible to determine a priori the consequences of the heat straightening on a specific steel; rather, they must be experimentally obtained on a case by case basis. Regardless of this, the experimental results reported in this study allow different families of steels to be distinguished and, from this, the following set of general recommendations to be stated: In general, when the critical (T_{Ac3}) / intercritical (between T_{Ac1} and T_{Ac3}) temperature is reached, the subsequent cooling rate must be controlled to avoid the formation of martensite. In addition, in order to prevent the formation of tertiary cementite in low carbon ferritic-pearlitic steels, low cooling rates below 650 °C must be avoided.

The conventional treatises recommend not exceeding the critical temperature of dissolution of pearlite to avoid the possible harmful consequences of the flame straightening treatment. The literature, however, makes no reference to the particular characteristics of the material or heat treatment such as cooling rate. This work has revealed the importance of these and other aspects and how, in some cases, the general recommendations lead to undesirable results.

Acknowledgments This paper describes the work performed by the Laboratory of the Division of Science and Engineering of Materials (LADICIM) of the University of Cantabria within the project OPTISTRAIGHT (Optimization and improvement of the flame straightening process, Contract N°: RFSR-CT-2007-00040). This Project was carried out with the financial grant of the Research Programme of the Research Fund for Coal and Steel; technical contributions from the members of the OPTISTRAIGHT members and the financial contribution from the Research Fund for Coal and Steel are gratefully acknowledged. The authors would also like to express their particular gratitude to the technical staff of DEGIMA S.A. and, specially, to Mr. Luis San Segundo, without whom it would have not been possible to conduct the experimental part of the present research.

References

1. Avent RR (1989) Heat-straightening of steel: fact and fable. JStructural Eng 115(11):2773–2793
2. Avent RR, Mukai DJ, Robinson PF (1998) Heat-straightening repairsof damaged steel bridges, a technical guide and manual of practice. Report No FHWA-IF-99-004,Federal Highway Administration, USA
3. Avent RR, Mukai DJ (2000) Heat-straightening rolled shapes, a technical guide and manual of practice. J Structural Eng 126(7):755–763
4. Avent RR (1995) Engineered heat straightening comes of age.Mod Steel Constr 35(2):32–39
5. Avent RR (1992) Designing heat straightening repairs, Proc. Nat. Steel Constr Conf, American Institute for Steel Construction (AISC)
6. Kumar AS, Kumar BR, Datta GL, Ranganath VR (2010) Effect ofmicrostructure and grain size on the fracture toughness of a microallowed steel. Mater Sci Eng, A 527(4–5):954–960
7. Ray PK, Ganguly RI, Panda AK (2003) Optimization of mechanical properties of an HSLA-100 steel through control of heat treatment variables. Mater Sci Eng, A 346(1–2):122–131
8. Yaowu S, Zhunxiang H (2008) Effect of weld thermal cycle onmicrostructure and fracture toughness of simulated heat-affected zone for a 800 MPa grade high strengh low alloy steel. Mater Sci Eng, A 207(1–3):30–39
9. Machado IF (2006) Technological advances in steels heat treatments. Mater Sci Eng, A 172(2):169–173
10. European structural steel standard EN 10025: 2004 Part 2—Technical delivery conditions for non-alloy structural steels
11. European structural steel EN 10025: 2004 Part 4—Technical delivery conditions for thermomechanically rolled weldable fine grain structural steels
12. European structural steel EN 10025: 2004 Part 6—Technical delivery conditions for flat products of high yield strength structural steels in the quenched and tempered condition
13. Bain EC, Paxton HW (1961) Alloying elements in steel, Americansociety for metals

14. Heat treating (2004) 10th ed. In: ASM Handbook Vol. 4. ASMinternational, Ohio
15. ANSYS user′s manual. Release 14; 2011
16. Moshiov A, Lattore R (1985) Temperature distribution duringplate bending by torch flame heating. J Ship Res 29(1):1−11
17. Lee JH (1995) Relations between input parameters and residualdeformations in line heating process, Ph.D. Thesis, Department of Naval Architecture and Ocean Engineering, Seoul National University, Seoul, Korea
18. Rykalin NN (1960) Calculation of Heat Process in Welding,Mashinostroenije Moscow
19. Manca O (1995) Quasi-steady-state three-dimensional temperaturedistribution induced by a moving circular Gaussian heat source in a finite depth solid. J Heat Mass Trans 38(7):1305−1315
20. Metallography and Microstructures (2004) tenth ed. In: ASMHandbook Vol. 9. ASM international Ohio, pp 598
21. Degarmo EP, Black JT, Kohser RA (2003) Materials and Processesin Manufacturing, 9th edn. Wiley
22. Pero-Sanz JA (2004) Aceros: metalurgia física, selección y diseño,Dossat 2000. Cie, S.L
23. ASTM E8-04 (2005) Standard Test Methods for Tension Testing ofMetallic Materials. In: Annual Book of ASTM Standards, vol 03.01. ASTM, Philadelphia
24. ASTM E23-01 (2005) Standard test methods for notched barimpact testing of metallic materials. In: Annual Book of ASTM Standards, vol. 03.02 [section 3]. ASTM, Philadelphia
25. Anderson TL (1995) Fracture Mechanics, Fundamentals andApplications, second ed., CRC Press
26. Kanninen MF, Popelar CH (1985) Advanced Fracture Mechanics,Oxford University Press
27. Rice JR (1968) A path independent integral and the approximateanalysis of strain concentration by notches and cracks. J Appl Mec 35:379
28. ASTM E1820-01 (2005) Standard Test Method for Measurementof Fracture Toughness. In: Annual Book of ASTM Standards, vol. 03.02 [section 3]. ASTM, Philadelphia
29. G. Krauss (1997), STEELS: Heat treatment and processing principles. ASM international